EUROPEAN ORGANIZATION FOR NUCLEAR RESEARCH

ATLAS Internal Note
TILE-CAL-NO-68
23 November 1995

The Muon energy losses in the Tile calorimeter

A. Henriques
LIP Lisbon, Portugal

G. Karapetian [1]
CERN, Geneva, Switzerland

A. Solodkov [2]
IHEP, Protvino, Russia

Abstract

We report on a study of high energy muons traversing the ATLAS hadron Tile calorimeter in the barrel region in the energy range between 2 and 300 GeV. Both, experimental data and MC simulations are presented showing good agreement. The capability of the Tile calorimeter in detecting isolated muons over the above energy range has been studied. A signal to background ratio of 10 to 1 is expected for nominal luminosities ($10^{34} cm^{-2} sec^{-1}$) at the LHC. The energy loss of a muon in the calorimeter, which is dominated by the energy lost in the iron, can be correlated to the energy loss in the scintillator. This correlation will allow to correct to an event-to-event basis the muon energy loss in the calorimeter and reduce the low energy tails on the muon momenta distribution.

[1] on leave from Yerevan Physics Institute, Armenia
[2] present address: LPC Clermont–Ferrand, Université Blaise Pascal / CNRS–IN2P3, France

1 Introduction

Although the main task of an hadron calorimeter is not to detect muons, the ATLAS Tile calorimeter can provide useful information on this subject.

Muons exceeding energies of 2 GeV will be measured in the ATLAS detector with a system of chambers placed inside an air core toroid after more than 100 radiation lengths of electromagnetic and hadronic calorimetry [1]. The design performances of the muon spectrometers in ATLAS are : $\Delta p_T/p_T = 2\%$ at 50 GeV and about 10% at 1000 GeV, see Fig. 1 [1], [2]. The fluctuations of the energy loss from the absorber material in a calorimeter in front of the muon spectrometer will limit the precision of the muon momentum measurement for p_T below 100 GeV. In general these fluctuations are reduced when the calorimeter absorber is made out of low Z material, like iron, as it is the case for the ATLAS Tile calorimeter, compared to lead or uranium. In ATLAS the energy loss in the calorimeters will dominate the muon momentum resolution in the muon spectrometers below 100 GeV. Above 100 GeV multiple scattering in the muon chambers and measurement errors will dominate [1].

At low muon transverse momenta, p_T, (muon p_T's between 2 and 5 GeV) calorimetric measurements become important, because a significant fraction of the muon energy will be absorbed in the calorimeter. In this energy range Monte Carlo simulations show that calorimeter information could be very useful to identify muons from B-mesons ($B^0 \rightarrow J/\Psi K^0$ with the subsequent decay of the $J/\Psi \rightarrow \mu^+\mu^-$). The idea has been to use the fact that very little energy will be deposited in the last sampling compartment in depth (after 8 interaction lengths) by light quark and gluon jets and minimum bias events, in constrast to muons [3]. This property can be used to identify muons as it has been demonstrated in Ref. [3].

In the muon momentum range of 10 to 100 GeV the use of the correlation between the energy loss in the scintillator and the energy loss in the iron could be interesting to correct the total amount of energy loss of a muon traversing the full calorimeter depth. This would allow to improve the muon momentum measurement in the spectrometers. The detection of the Higgs boson in its intermediate mass range via the decay channel $H \rightarrow ZZ^* \rightarrow 4\mu$ would profit from such an improved muon momentum measurement.

The light yield produced by muons in a scintillator is usually very small compared to signals from particles for which the calorimeter system was constructed for. The additional request to also identify muons with the Tile calorimeter puts further constrains on the dynamical range of the readout system. Low noise and high photoelectron statistics are additional important ingredients to perform well the energy deposited by muons.

All these aspects have been studied and investigated with two prototype setups in test beams using muons at energies between 10 and 300 GeV and incident polar angles between 0^o and 90^o. In addition, MC simulations have been

performed for muons of energies between 2 and 300 GeV.

The present paper is organized as follows: Section 2 describes the test beam setup, the data taking and the selection procedures. The test beam and MC results are discussed in Section 3. Finally some conclusions are given in Section 4.

2 The Test Beam Setup

Two different setups have been used to test the prototype modules in test beams at the CERN-SPS.

In the stand-alone mode the Tile calorimeter modules have been positioned on a scanning table, able to allow high precision movements along any direction in space (z, θ, ϕ). The Tile calorimeter prototype consists of five 1 m long modules with a front face of 100×20 cm^2, each module spanning $2\pi/64$ in azimuth. The radial depth is 180 cm, starting at an inner radius of 200 cm up to an outer radius of 380 cm corresponding to 8.9 interaction lengths (λ) at $\eta = 0$ or to 80.5 radiation lengths (X_0). Each module has 57 identical scintillator tiles of 3 mm thickness along z and 18 tiles, each of different dimension, in radial depth. Within one module the readout fibers are regrouped to define a cell granularity of $\Delta\eta \times \Delta\phi \simeq 0.1 \times 0.1$. The calorimeter is radially divided into four depth segments by grouping fibers from different tiles. Beam chambers and beam defining elements have been placed just in front of the scanning table. A large scintillator wall covering about 1 m^2 of surface has been placed on the side and on the back of the calorimeter to quantify back and side leakage of hadronic showers.

Muons with energies between 10 and 300 GeV have been shot on the calorimeters at incident polar angles between 0^o and 90^o [5].

For the combined run (TILECAL+LAr) the test beam setup has been different. It is shown in Fig. 2. The Tile calorimeter has been placed on a fixed table, just behind the LAr Accordion cryostat. Both the cryostat and the Tile calorimeter have been tilted with respect to the beam axis by $\theta = 11.3^o$. This combined test was mainly dedicated to study the calorimeter response to hadrons, but muons of energies between 20-300 GeV were also available from muon contamination in pion beams [5]. A dedicated muon beam of 300 GeV could also be used.

For the LAr electromagnetic calorimeter the large 2 m prototype [6] of RD3 has been used, located close to the back of the cryostat to reduce the distance between the two active devices. In this layout the effective distance between the two devices is of the order of 45 cm, instead of the 25 cm as foreseen in the ATLAS setup. The amount of material has been quantified to be about $2X_0$ in between the two calorimeters. This value is similar to the ATLAS design value, but the material type is different: steel instead of aluminum for the cryostat.

The 2 m LAr electromagnetic calorimeter prototype which has full projective

geometry consists of a stack of three azimuthal modules covering 27^o in ϕ. The segmentation is $\Delta\eta \times \Delta\phi \simeq 0.018 \times 0.02$ for the first two compartments (each having 9 X_0 in depth) and $\Delta\eta \times \Delta\phi$ simeq 0.036×0.02 for the last one (7 X_0).

Beam elements and beam chambers in front of the cryostat are used to define the beam position and its quality.

For this study only the 2 most energetic cells in each longitudinal sampling of the LAr and the Tile calorimeters have been used to reduce the contamination from electronics noise. The results from the Tile calorimeter stand-alone beam tests show that a muon looses energy in only one cell per longitudinal depth.

3 Results

3.1 Effect of photoelectron statistics on the signal shape

The energy loss measured in the Tile calorimeter from 150 GeV muons at a polar angle of $\theta = 10^o$ is shown in Figs. 3a and 3b for the full calorimeter depth (9 λ) and for the first longitudinal sampling (1.5 λ) only. The energy loss spectrum follows approximately a Landau distribution, but with large tails at high energies due to the electromagnetic shower component (Bremsstrahlung, electron-positron pairs, energetic knock-on electron production). The experimental data have been converted to GeV using the calibration constants obtained from the calorimeter response to electrons (5.59 pC/GeV).

The energy loss deposited in the scintillator obtained from MC simulation is also shown in Fig. 3 with and without experimental effects have been taken into account, coming from i.e. fibre/tile fluctuations, PMT noise and photoelectron statistics. The MC simulations agree well with experimental data when these experimental effects have been taken into account. The broadening of the distribution due to the photoelectron statistics is mostly seen in the first sampling, which is the thinnest compartment of the Tile calorimeter (30 cm or 1.5 λ). The MC data have been normalized to the experimental data at 50 GeV to obtain the same most probable value of energy loss.

The pedestal distribution after subtraction of its average value is also shown in Fig. 3. The width of this distribution, corresponding to a noise of about 40 MeV/cell (2 PMT's), is very small. Therefore the pedestal is well separated from the muon signal. The signal in the first sampling is collected with two PMT's only, whereas the total signal is the sum of 10 PMT's (one cell in sampling 1, 2, 4 and 2 cells in sampling 3). The broadening of the spectrum of the muon energy loss due to photoelectron statistics was also observed experimentally.

The energy loss of muons with 150 GeV incident energy traversing the calorimeter at a polar angle $\theta = 10^o$ corresponding to an effective depth of 9 λ is shown in Fig. 4 for the three different Tile calorimeter prototypes with the light yield values of 24 pe/GeV, 48pe/GeV and 64 pe/GeV, respectively [5]. The broad-

ening of the spectrum of the muon energy loss is clearly visible when only the first longitudinal sampling is taken into account. Only a small broadening of the width of the muon line shape is observed for the module with 24 pe/GeV when integrating over the full Tile calorimeter depth. This indicates that a further increase of the light yield above 64 pe/GeV would not improve the quality of the muon measurements. Nevertheless, ageing effects and radiation damage will reduce the light yield and in long term the calorimeter performance will profit from the highest light output.

3.2 Energy dependence of the muon response

The energy loss in the calorimeter has been studied with muons traversing the stand-alone Tile calorimeter at a polar angle of $\theta = 10^o$ for both, experimental data and for MC simulations (all instrumental effects included), at energies between 10 and 300 GeV. The MC simulations include also muon energies between 2 and 5 GeV. To be able to compare to experimental data, the MC simulations have been performed with the same spot size (1 cm), impact point and polar angle.

The energy loss measured in the Tile calorimeter is shown in Fig. 5 for both, experimental data and MC simulations, for muon energies of 5 GeV (MC only), 20, 100 and 200 GeV, respectively. As expected, the most probable (peak) value increases gradually to larger values with increasing energy and the distributions get more pronounced tails. The later is due to the electromagnetic shower component (Bremsstrahlung, electron-positron pairs, energetic knock-on electron production) for high energy muons which is well reproduced by the MC. Both, the most probable (peak) value of the energy loss and the average value truncated at 5σ above the peak value have been calculated. The peak values have been obtained from a fit of the energy loss distributions to a Moyal function [7].

The average and the peak values for the energy loss measured in the Tile calorimeter (8.9 λ) as a function of the muon beam energy for a polar angle of $\theta = 10^o$ is shown in Fig. 6 and in Table 1. On average a muon deposits 2.7 GeV of its energy in the scintillator of the Tile calorimeter. The most probable energy loss increases by approximately 7% per 100 GeV/c increase in muon momentum over the range of 50 to 300 GeV/c. The truncated mean increases more steeply, approximately 10% per 100 GeV/c increase in muon momentum. Also shown is the most probable value for the energy loss measured in the combined TILECAL-LAr calorimeters (10.1 λ or 106 X_0). As expected, the LAr calorimeter adds little to the total energy loss of muons, about 4% (15%) of the total signal for 20 (300) GeV muons, because the LAr calorimeter amounts to only 24% of the total material of calorimeters in X_0 units ($25X_0$ out of $106X_0$). On the other hand the lower noise level in the hadronic calorimeter (40 MeV/cell instead of 70 MeV/cell for the LAr calorimeter [5]) allows a better determination of the energy loss of a muon, because it depends less on pedestal fluctuations. The use

of the the muon information in the electromagnetic calorimeter is maybe possible as can be seen from test beam data in Fig 7. Further studies should be continued.

For all results presented in the following, only the energy loss in the Tile calorimeter has been used.

The average muon energy deposition in the scintillator of the Tile calorimeter of about 2.7 GeV can be compared to the expected energy deposition of minimum bias events per bunch-crossing for nominal luminosities ($10^{34} cm^{-2} sec^{-1}$) at the LHC, which amounts to $\sim$ 0.2 GeV into a $\Delta\eta \times \Delta\phi = 0.1 \times 0.1$ calorimeter cell. This gives a comfortable margin for detecting isolated muons in the Tile calorimeter, even at the highest luminosity (S/B $\sim$ 10).

3.2.1 Fluctuations of the muon energy loss in Tile calorimeter

MC studies show, as already mentioned in the previous Section, that the electromagnetic shower component (Bremsstrahlung, electron-positron pairs, energetic knock-on electron production) for high energy muons produce large tails in the spectrum of the energy loss. Fig. 8 shows the energy deposition in the iron as a function of the energy deposition in the scintillator for different incident muon energies (no correction for the sampling fraction has been made). This energy loss in the scintillator due to the electromagnetic shower component is highly correlated to the energy loss in the absorber material as can be seen in Fig. 8. This correlation is already visible for muon energies above 10 GeV. Below this value no correlation exists because of pure ionization mechanisms.

Fig. 9 shows the average values of the energy loss in iron as a function of the average energy loss in the scintillator for 300 GeV muons. The functional behaviour can be parameterized with the following formula, which is superimposed on Fig. 9:

$$E_{Fe} = a_1 \times E_{Sc}^{-a_2} + p_1 \times E_{Sc}^{p_2}, \quad (1)$$

where p_1, p_2 are polynomial functions with

$$\begin{aligned} p_1 &= a_3 + a_4 \times E_\mu \\ p_2 &= a_5 + a_6 \times E_\mu + a_7 \times E_\mu^2, \end{aligned}$$

where a_n $(n = 1 \ldots 7)$ are constants and E_μ is the incident muon energy in GeV.

This parameterization could be used to correct for the energy loss in the calorimeter and improve the momentum measurement in the muon spectrometers. In the ATLAS environment due to variations of the fraction of dead and active

material such a parameterization would have to be evaluated for each muon impact point as a function of z and pseudo-rapidity η.

The same functional behaviour exists for the MC results between 10 and 300 GeV of incident muon energy as shown in Fig. 10. One observes that for a certain energy deposited in the scintillator the energy deposited in the iron is almost independent of the incident muon energy. Table 2 shows the spread (RMS) of this correlation as a function of the energy deposited in the scintillator when all muon energies except 5 GeV are taken together. The RMS is equal to 359 MeV for $E_{scint} \leq 80$ MeV. This spread increases gradually with the energy deposited in the scintillator up to 2 GeV for 250 MeV $\leq E_{scint} \leq 5$ GeV.

A more detailed study has been done for each incident muon energy. The spread of the correlation of the energy loss in Fig. 8 for each incident muon energy gives a hint about the precision to which the energy loss in iron can be estimated using the energy loss in the scintillator at an event to event basis. The difference of the energy loss in the Tile calorimeter absorber and the energy loss in the scintillator is shown Fig. 11. This difference has been corrected for the sampling fractions in iron (1-f) and in scintillator (f), respectively, adjusted such that the mean value of the difference is zero. The value of f$\sim$ 3% varies very little with the muon energy, see table 3a.

With increasing muon energies high energy tail are observed in the distributions of Fig. 11. The fraction of events in the tail above a 3 σ cut are 1% at 10 GeV and about 5-6% for muon energies above 150 GeV, as summarized in Table 3a. Figs. 12a and 12b show the difference of the energy loss for 300 GeV muons as a function of the energy deposition in the scintillator and as a function of the energy deposition in the iron, respectively. As can be seen from this Figure, these less correlated events deposit an enormous amount of energy in both, the iron and the scintillator, probably due to catastrophic energy loss, where the muon losses nearly all its energy in the iron.

A Gaussian fit within $\pm 2\,\sigma$ has been performed and its result is superimposed on each of the distributions in Fig. 11. The sigma of the Gaussian fit (in MeV) is shown in Fig. 13a (black dots) and in Table 3a as a function of the incident muon energy. The width divided by the incident muon momentum as a function of the incident muon energy is shown in Fig. 13b (black dots).

At high muon momenta (above 100 GeV) the σ value amounts to about 400-500 MeV (0.2-0.3%). The precision profits from the relative low Z absorber material (iron) used in the Tile calorimeter. In this energy range the muon momentum resolution in the ATLAS muon spectrometers is dominated by multiple scattering in the muon chambers and by the measurement error including contributions from chamber alignment [1].

In the TILECAL-LAr combined test, with 1.2 λ or 25 X_0 of electromagnetic (Pb/LAr) calorimetry in front, these fluctuations stay at the same level, because the electromagnetic compartment adds little to the total depth of calorimetry. If, for example, the absorber material would be made out of lead only, the fluc-

tuations of the energy loss in the calorimeter are expected to be much larger for a calorimeter having about the same depth in λ units and the same sampling fraction [4].

For muon momenta below 100 GeV the value of *sigma* increases rapidly up to 3.1% (310 MeV) for 10 GeV and 5.9% (295 MeV) for 5 GeV. In ATLAS for energies below 10 GeV the muon momentum resolution does not depend anymore on the quality of the muon spectrometer placed behind the hadron calorimeter.

In summary, the precision of the correlation E_{Fe} versus E_{scint} is found to be of the same order of the fluctuations of the energy loss in the calorimeter as can be seen in column 2 and 6 of Table 3a.

The precision on the determination of the muon energy loss in the ATLAS calorimeter system will be worse, because of effects described in the following.

In the ATLAS environment there will be 107 X_0 (10.6 λ) of material in front of the muon spectrometer at $\eta = 0$. This corresponds to 1.15 X_0 from the inner tracking, the cryostat, the solenoid and the presampler in front of the electromagnetic calorimeter, 25 X_0 from the LAr calorimeter itself, 2 X_0 from the cryostat wall between the electromagnetic and hadronic calorimeters, 68.7 X_0 from the Tile calorimeter and 9.7 X_0 from the girder structure of the Tile calorimeter (see Table 4). Assuming that only the Tile calorimeter will be able to detect muons, there will be only 64% of 107 X_0's to sample actively the muon energy loss. In addition, the LAr calorimeter amounts to only 24% of the total material and with a high Z absorber material, lead instead of iron. Therefore, it is expected that the determination of the energy loss of muons will be $\sim$ 30% worse, if the analysis is restricted to the amount of absorber material of the Tile calorimeter only.

This worsening in the determination of the energy loss has been estimated with the MC program of the Tile calorimeter prototype using the fact that the muon looses energy in the full calorimeter depth (80.5 X_0), but only 67% of the total energy loss is seen by the Tile calorimeter. This configuration is very close to the ATLAS environment at $\eta = 0$. The results of the simulation are shown in Figs. 13a and 13b (open circles) and Table 3b. A worsening of the resolution of 32% (29%) for 5 GeV (300 GeV) muons is observed. It does not depend much on the muon momenta.

For muon energies of 10 GeV and 300 GeV the worsening in the determination of the energy loss has been studied as a function of the active sampling fractions with respect to the total energy loss in the calorimeters as shown in Fig. 14. As expected, the determination of the energy loss degrades with smaller active sampling fractions. This degradation will be of the order of 30-40% in ATLAS were the Tile calorimeter amounts to 64% of the total calorimetry.

From the geometrical construction of the Tile calorimeter one expects a modulation of the muon energy loss along the z direction, in particular for polar angles close to zero, for both, the energy deposition in iron and in the scintillator, but the later displaced in z by half a period (4.5 mm). To avoid effects due to this

structure in the present Section all results on the energy loss have been simulated with a fixed impact point of 1 mm diameter instead of 1 cm. This modulation effect is indeed seen in the MC as illustrated in Fig. 15 for 180 GeV muons entering the Tile calorimeter at $\theta = 0^o$. The impact points with the maximum signal in iron correspond to the places with a minimum signal in the scintillator (anticorrelation). The signal period of 9 mm precisely reproduces the staggered tile/iron geometry. This effect has also been observed with test beam data.

The fluctuations of the energy loss will affect the momentum measurement and degrade the resolution, if no correction is applied. In the ATLAS environment the muon impact point and its polar angle will be known from the inner tracking detectors. With this knowledge the exact amount of iron and scintillator seen by the muon track can be determined and corrected for.

3.2.2 The muon momenta resolution after correcting for the energy loss fluctuations

The improvement of the muon momenta resolution in the ATLAS muon spectrometer after correcting for the energy loss fluctuations in the Tile calorimeter prototype (80.5 X_0 fully sampled) was estimated for 20 GeV muons.

Three different methods were applied. The first method adds to each event the most probable value of the energy lost by muons in the calorimeter (peak = 2.32 GeV for 20 GeV muons, see Table 1).

The results are shown in Fig. 16a. As expected the distribution peaks at the correct energy value but a low energy tail exists. A smearing of this distributions was done with an energy dependent function which describes the contribution of the multiple scattering and the measurement/alignment error in the muon chambers (quadratic sum of dashed and doted lines in Fig. 1, Ref. [1]). The results are shown in Fig. 16b. A gaussian fit between within ± 2 σ has been performed and its result is superimposed to the distribution. The sigma of the Gaussian fit is 349 MeV and the percentage of events below 3 *sigma* amounts to 7%.

The second method corrects on the event-to-event basis for the energy loss in the calorimeter ($E_{Fe} + E_{scint}$). This method already described, uses as information the energy loss in the scintillator and the estimated energy loss in the iron. For this estimation the parameterization of eq. 1 is used. The results are shown in Fig. 16c before smearing. The events on the low energy tail mostly disappear. The same distribution after smearing for the contribution of the beam chambers is shown in Fig. 16d. The sigma of the Gaussian fit is similar to the value obtained with the first method (356MeV or 1.8% instead of 349 MeV) but the percentage of events which remain in tails after smearing is much lower with the correction on the event-to-event basis (1.7% instead of 7%). In ATLAS technical proposal (Fig. 1) the momentum resolution estimated is 2.3% for 20 GeV muons. This difference comes from the bigger contribution attributed to the energy loss

fluctuations in the calorimeter.

A third correction which is a mixture of the 2 first methods was considered: events which deposit little energy in the calorimeter ($E_{scintillator} \leq 80$ MeV, see Fig. 10) are corrected with the most probable energy loss (first method), the events which are in the high energy tail of the signal ($E_{scintillator}$ above 80 MeV) are corrected for the estimated energy loss on the event-to-event basis (second method). The results are shown in Fig. 16e before smearing and Fig. 16f after smearing. A very similar result is obtained comparing with method 2. The momentum resolution does not change and the tails are recovered to the 1.4% level.

The same study has been done for 300 GeV muons, see results in Fig. 17. For high energies the contribution of the multiple scattering and the measurement alignment error in the muon chambers dominate the muon momentum resolution as can be seen in Fig. 1. The effect of the correction on the event-to-event basis is not so important as for low energy muons due to the almost inexistent tails in the momentum distribution after smearing (about 1% tails).

The results shown up to now are optimistic in the sense that in the ATLAS detector a fraction of the calorimeter material traversed by muons is not sampled. This is the case for the energy deposited in the girder structure and maybe in the electromagnetic calorimeter which sums 36% of the total material in terms of X_0s.

This study was repeated considering that the last sampling of the Tile calorimeter is not sampled by the scintillator (only 67% of calorimeter active), situation close to the ATLAS setup if the electromagentic information is not taken.

The results for 20 GeV muons are shown in Fig. 18. There is not observed any significant deterioration on the muon momenta resolution but an increase of the amount of tails (about 5% instead of 2%). Those additional tails should be recovered in ATLAS at least partially using the information of the electromagnetic calorimeter (25 X_0s). Those events would deposit a lot of energy in the em calorimeter, the less affected region by pedestal fluctuations, see Fig. 7.

In summary this study shows that the correction of the energy loss in the calorimeter on the event-to-event basis should be done for the events which deposit a lot of energy in the calorimeter in order to reduce the low energy tails observed in the muon momentum distribution. There is no improvement but neither degradation of applying such a correction on the events which deposit energy close to the most probable value of the muon signal. This is because the precision of the correlation $E_{scintillator}$ versus E_{iron} is of the same order of the width of the energy loss fluctuations in the calorimeter. The parametrization used in this study was optimized to fit the correlation in the full energy range. In case of using the correction only for the events wich deposit a lot of energy in the calorimeter the parameterization can be certainly simplified. The parametrisation with only one coefficient, which is the slope of the distribution at Fig. 10, or in other words the muon sampling fraction (f) can be used. If this simpler

correction is applied very similar results to those shown in 16e,f are obtained. This simpler method has also the advantage that the muon sampling fraction is more or less constant for all muon energies (see Table 3). f will have anyway to be corrected for the muon impact point and angle as seen in Fig. 15.

4 Conclusions

The capability of detecting isolated muons in the energy range 2 to 300 GeV with the Tile calorimeter has been studied. A signal to background ratio of 10 to 1 is expected for nominal luminosities ($10^{34} cm^{-2} sec^{-1}$) at the LHC.

The muon energy loss in the calorimeter, which is dominated by the energy loss in iron can be recovered at an event-to-event basis using the energy loss in the scintillator. This may be possible for muon energies above 10 GeV due to the correlation between the energy deposited in iron and scintillator.

The resolution of the estimation of the energy loss in the calorimeter is about 400-500 MeV (0.2-0.3%) for muon energies above 100 GeV. For energies below 100 GeV the resolution increases rapidly up to 310 MeV (3.1%) for 10 GeV and 295 MeV (5.9%) for 5 GeV muons.

A worsening of about 30% is expected in the ATLAS environment if only the Tile calorimeter will be used in the full calorimeter system to sample the muon signal before the muon spectrometer. The possibility to extract the muon information from the electromagnetic calorimeter has to be investigated further.

This method gives about the same momentum resolution as the standard technique of correcting for a mean energy loss in the calorimeter. Nevertheless the correction on the event-to-event basis ables to reduce the amount of events in the low energy tail of the muon momentum distribution. If this correction is applied only to the events wich deposit a lot of energy in the calorimeter the correction used can be simplified. The parametrisation with only one coefficient, which is the muon sampling fraction can be used giving similar results. More studies are needed to estimate quantitatively such an improvement in a realistic ATLAS detector description.

This correction method should be studied in a real physics channel like the detection of the Higgs boson in its intermediate mass range via the decay channel $H \rightarrow ZZ^* \rightarrow 4\mu$.

Acknowledgements

We would like to thank H. Plothow-Besch and C. Fabjan for the careful reading and constructive comments on this note. Thanks to M. Cavalli, D. Froidevaux, M. Nessi and L. Poggioli for the valuable discussions. The authors are greatly indebted to all collaboration for the test beam setup and data taking. One of us (A. H.) would like to thank to Junta Nacional de Investigacão Científica of Portugal for the POS-DOC scolarship.

References

[1] ATLAS Technical Proposal, CERN/LHCC/94-43 LHCC/P2.

[2] Ph. Schune, C. Guyot and M. Virchaux, ATLAS Internal Note, MUON-NO-65 .

[3] D. Pantea et al., ATLAS Internal Note, TILECAL-NO-023 and TILECAL-NO-062.

[4] A. Acosta et al., Nucl. Instr. and Meth. **A320** (1992) 128.

[5] E. Berger *et al.*, CERN/LHCC 95-44, LRDB status report/RD34, 1995

[6] D.M. Gingrich at al. (RD3 Collaboration), RD3 Internal Note 58, to be submitted to NIM.

A. Bernstein et al., Nucl. Instr. and Meth. **A262** (1987) 229.

[7] E. Moyal, Phil. Mag. **46** (1955) 263.

List of Tables

List of Figures

Muon line shape characteristics						
	Exp		MC		Exp	
E_μ (GeV)	$peak_{had}$ (GeV)	$width_{had}$ (GeV)	$peak_{had}$ (GeV)	$width_{had}$ (GeV)	$peak_{had+em}$ (GeV)	$width_{had+em}$ (GeV)
2			2.06	0.47		
5			2.25	0.42		
10	2.29	0.51	2.30	0.50		
20	2.31	0.55	2.32	0.53	2.41	0.75
50	2.4	0.59	2.40	0.63	2.68	0.78
100	2.51	0.75	2.50	0.76	2.79	0.89
150	2.62	0.85	2.59	0.89	2.93	1.08
200	2.67	0.94	2.70	0.99	3.09	1.23
300	2.88	1.28	2.89	1.21	3.31	1.41

Table 1: The characteristics of the line shape of the energy loss measured in the active part of the Tile calorimeter (stand-alone test beam) and in the active part of the TILECAL+LAr calorimeters (combined test beam). The peak and width (in GeV) were obtained from a Moyal fit to the signal distributions truncated at $+5\ \sigma$. Experimental data are compared to MC simulations for stand-alone Tile calorimeter setup. Both the experimental and MC data have about the same spot size (1 cm diameter), impact point (centre of module) and polar angle ($\theta = 10^o$). The MC data have been normalized to the experimental data at 50 GeV.

The spread of the correlation E_{Fe} versus E_{sci} with all energies mixed	
$E_{scintillator}$	RMS (MeV)
$E_{scint} \leq$ 80 MeV	359
80 MeV $\leq E_{scint} \leq$ 150 MeV	652
150 MeV $\leq E_{scint} \leq$ 250 MeV	1207
250 MeV $\leq E_{scint} \leq$ 5000 MeV	2042

Table 2: The spread (RMS) of the correlation E_{Fe} versus E_{sci} with all muon energies between 10 and 300 GeV taken together as a function of the energy deposited in the scintillator.

Fluctuations of the muon energy loss in the Tile calorimeter

a) the full calorimeter depth ($80.5X_0$) is sampled by scintillator

E_μ (GeV)	σ (MeV)	σ/E_μ (%)	Number of events $\geq 3\ \sigma$ (%)	sampl. fraction. f (%)	*sigma* of E_{loss} (MeV)
5	295	5.90	0.4	3.02	228
10	310	3.10	0.9	3.01	272
20	318	1.59	1.6	3.04	281
50	342	0.68	2.6	3.00	360
100	377	0.38	4.3	2.96	539
150	420	0.28	4.7	2.93	637
180	441	0.25	5.2	2.90	751
200	432	0.22	5.5	2.87	821
300	525	0.17	5.8	2.83	1260

b) only 67% (54 X_0) of the scintillator signal is used

E_μ (GeV)	σ (MeV)	σ/E_μ (%)	Number of events $\geq 3\ \sigma$ (%)	sampl. fraction. f (%)	
5	391	7.82	0.1	2.01	
10	387	3.87	1.4	2.00	
20	394	1.97	3.6	2.01	
50	409	0.82	3.6	1.99	
100	492	0.49	5.0	1.97	
150	511	0.34	6.3	1.95	
180	589	0.33	6.5	1.93	
200	603	0.30	6.5	1.92	
300	676	0.23	9.4	1.87	

Table 3: The precision (σ in MeV and in percent of the incident muon energy) on how the energy losses in iron and scintillator can be estimated using as information the energy loss in scintillator. In column 6 are also shown the sigma of the fluctuations of the energy loss in the calorimeter taken from a Moyal fit. Results in Table (a) are obtained when the full calorimeter length is sampled by the scintillator ($80.5\ X_0$), (b) when only 67% of the calorimeter is sampled by the scintillator (the scintillator signal from sampling 4 was not acquired) but the muon still travels the full calorimeter length. The MC events were simulated in a spot of 1 mm, see text for details.

The amount of material downstream of the muon spectrometer for $\eta = 0$		
Component	thickness (λ)	thickness (X_0)
inner + cryost + presampler + Solenoid	0.3	1.15
LAr calorimeter	1.2	25
Cryostat	0.5	2
Tile calorimeter	7.6	68.7
Girder structure	1.0	9.65
total	10.6	106.7

Table 4: The amount of material in front of of the muon spectrometer for $\eta = 0$.

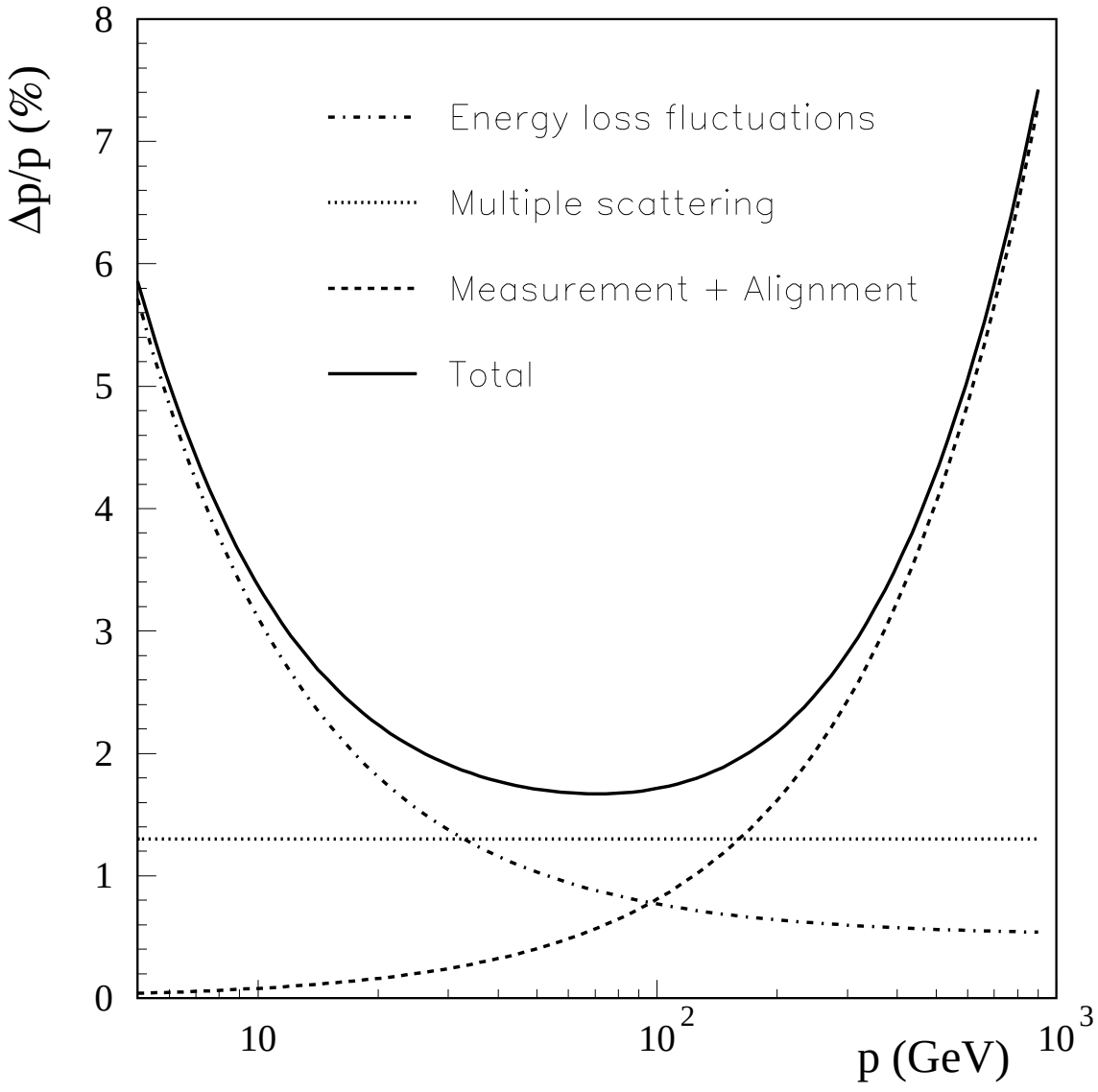

Figure 1: Momentum resolution at zero rapidity, as a function of the muon momentum. The figure shows the contribution from energy loss fluctuations in the calorimeter, multiple scattering in the precision and trigger chambers, and the measurement error including alignment contribution (Figure taken from ref. 1).

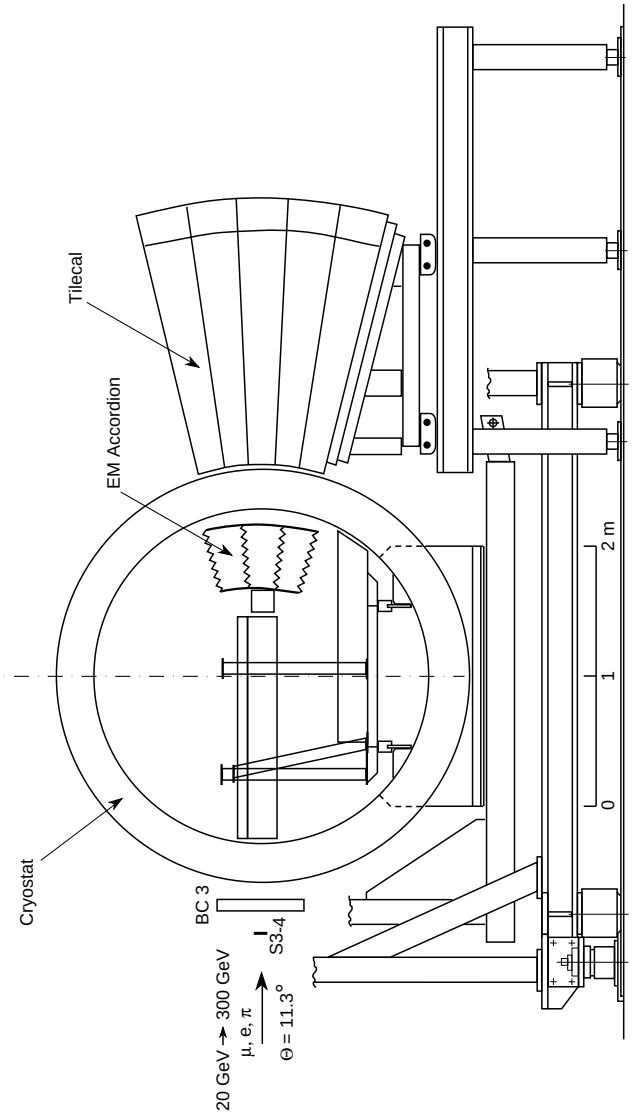

Figure 2: Test beam setup for the combined LAr and Tile calorimeter combined run

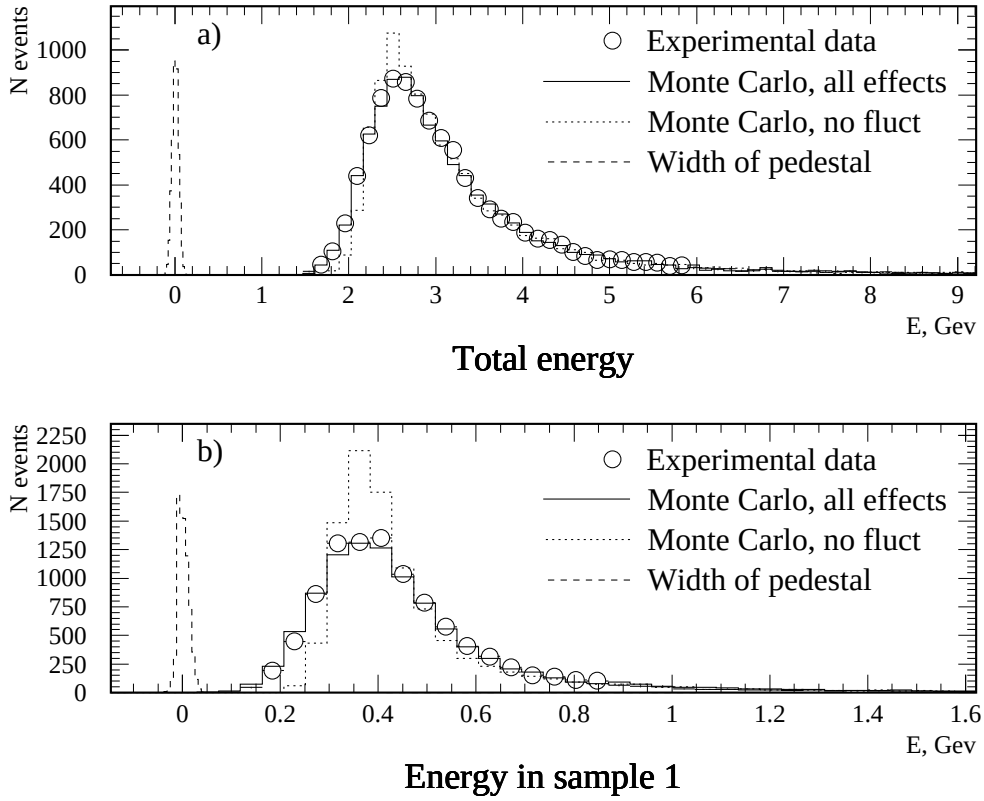

Figure 3: Energy loss measured in the active part of the Tile calorimeter for muons of 150 GeV muons traversing (a) the full Tile calorimeter depth (9 λ), (b) the first sampling (1.5 λ). The dotted points are experimental data while the dashed and full lines are MC results with and without experimental fluctuations, respectively. The pedestal width is also shown. Both the experimental data and MC simulation have about the same spot size (1 cm diameter), impact point (centre of module) and polar angle ($\theta = 10^o$).

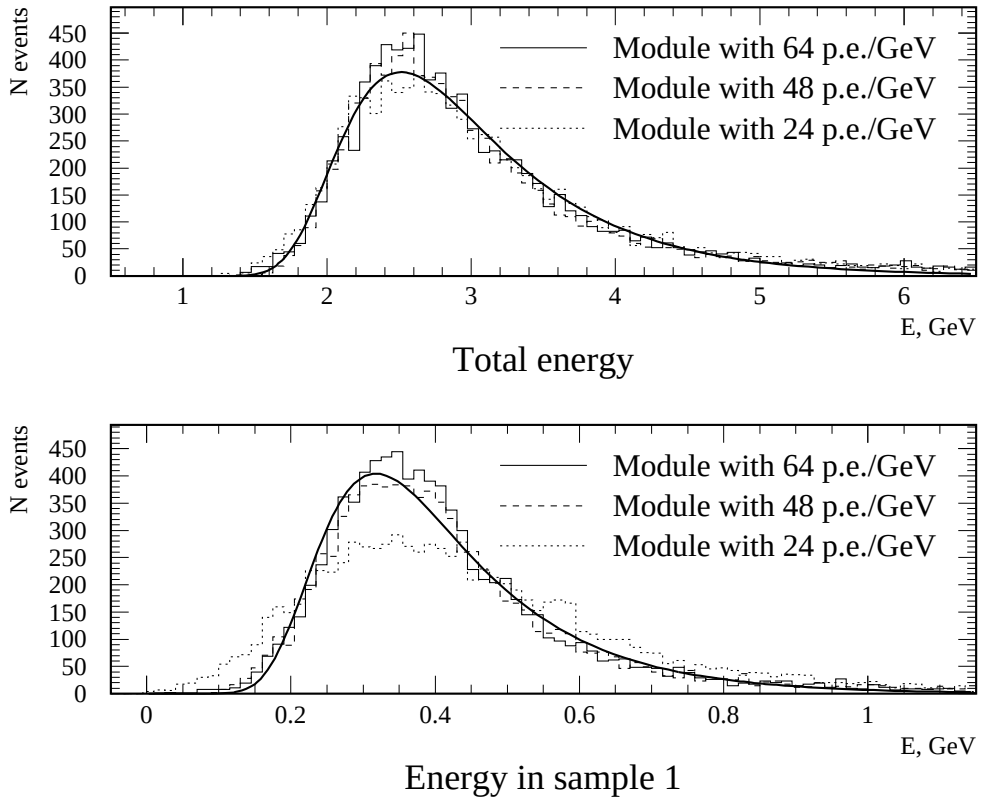

Figure 4: Energy loss measured in the Tile calorimeter for 150 GeV muons traversing (a) the full calorimeter length (9 λ), (b) the first sampling (1.5 λ) of three prototypes with different light yields (24, 48 and 64 pe/GeV per cell). A Moyal fit applied on the module with the highest light yield is show as a full curve.

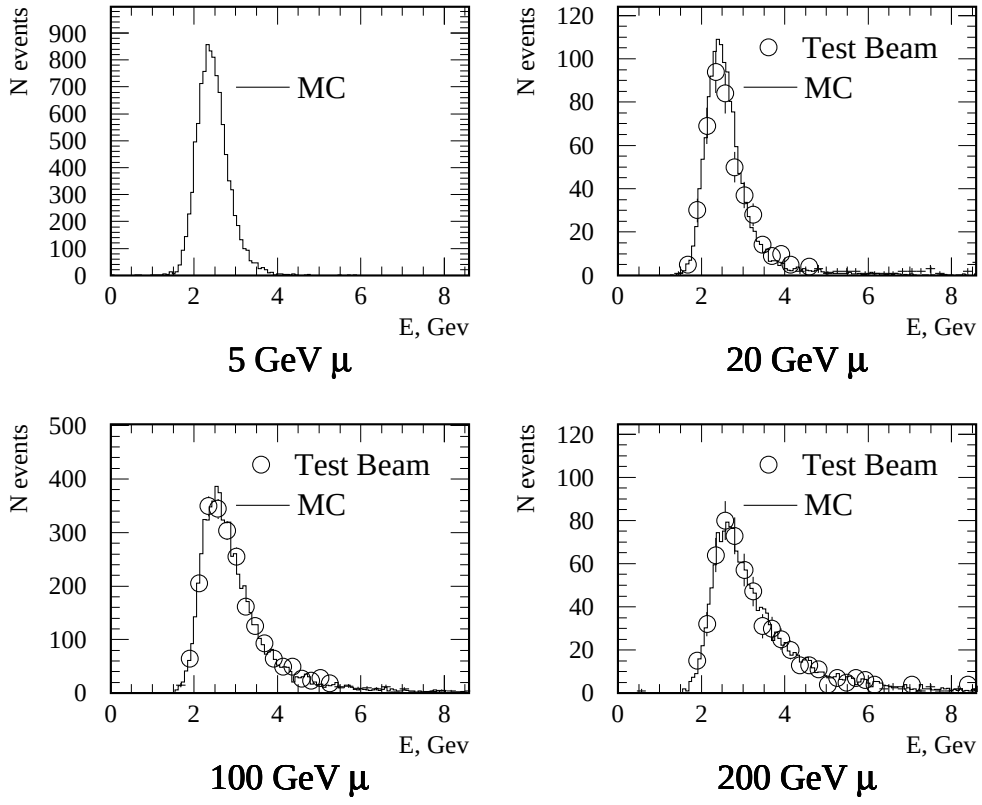

Figure 5: Energy loss measured in the Tile calorimeter from MC and experimental data for muons of 5 GeV (only MC), 20 ,100 and 200 GeV traversing the full Tile calorimeter length (9 λ). Plots are shown up to the peak plus 5 σ. Both the experimental data and MC simulations have about the same spot size (1 cm diameter), impact point (centre of module) and polar angle ($\theta = 10^o$).

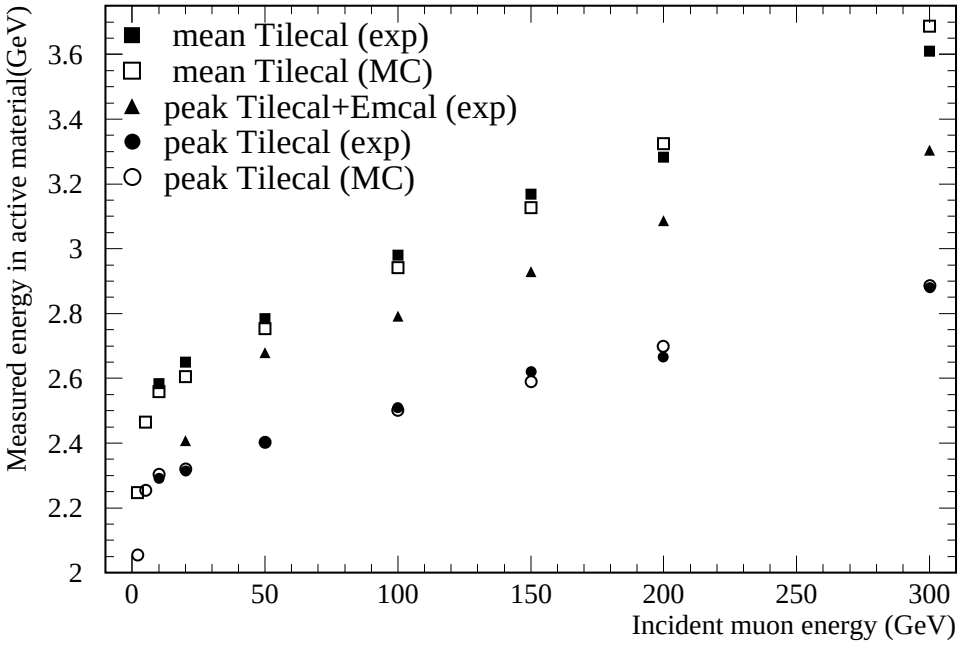

Figure 6: The truncated mean and the peak values for the energy loss measured in the Tile calorimeter as a function of the muon beam energy. Peak values are also given for the combined Tile+LAr test. Values have been calculated taking events depositing a signal up to the peak plus 5 σ. Both the experimental data and MC simulations have about the same spot size (1 cm diameter), impact point (centre of module) and polar angle ($\theta = 10^o$). See details in text.

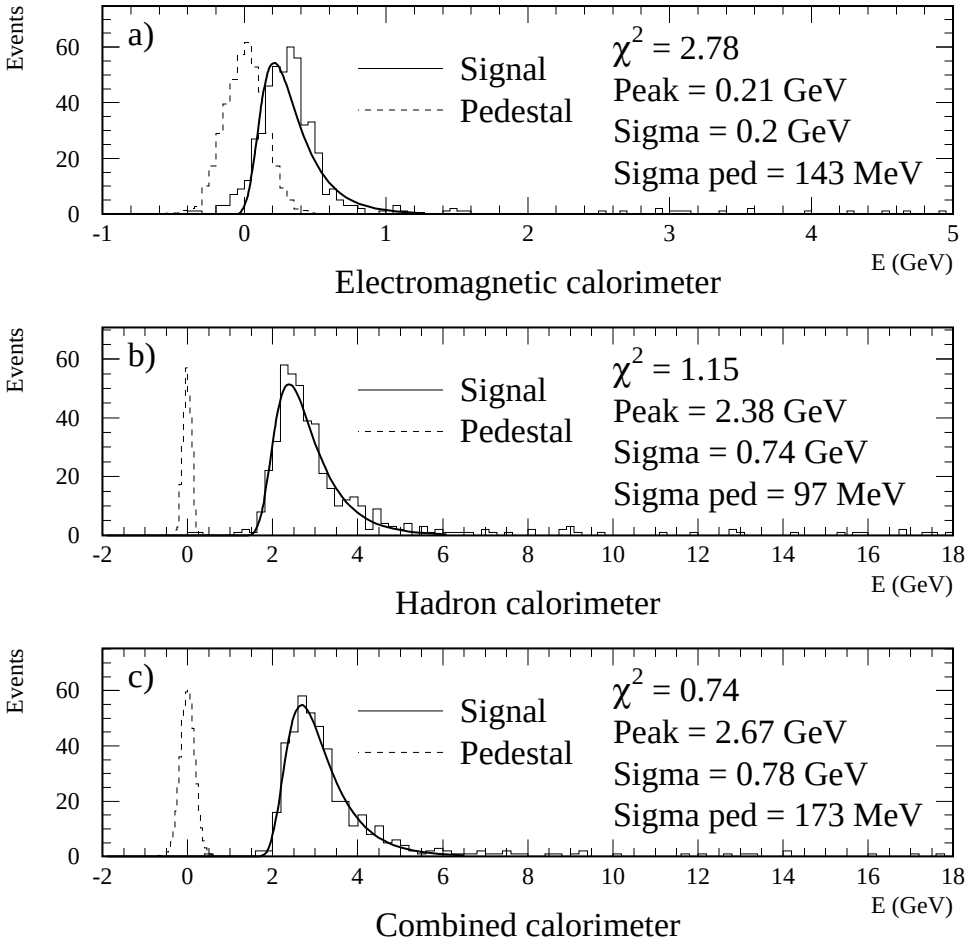

Figure 7: Energy deposited by 50 GeV muons in (a) the electromagnetic (LAr/Pb) calorimeter (b) in the hadronic calorimeter, (c) in the electromagnetic and Hadronic (Tile) calorimeters. The pedestal fluctuations of the cells used to collect the signal are also shown.

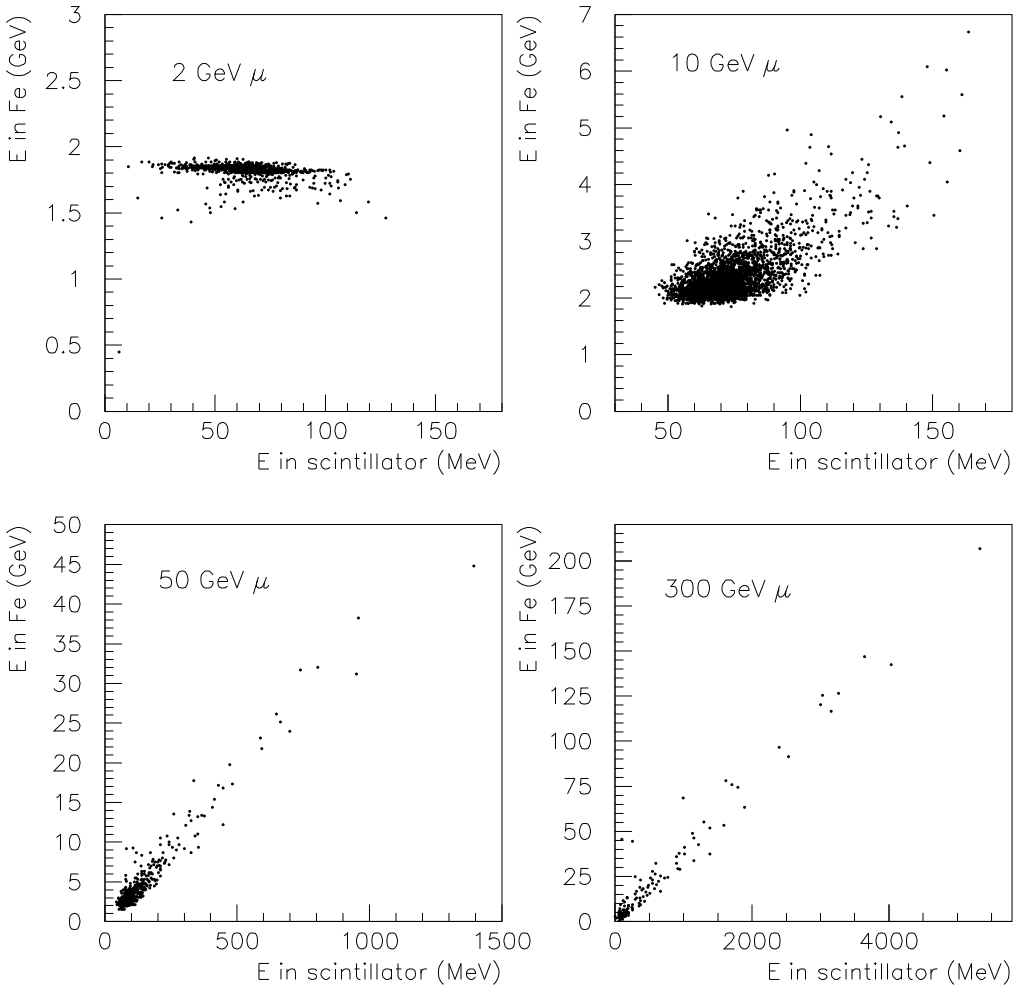

Figure 8: Energy loss in the scintillator (in MeV) as a function of the energy loss in the Tile calorimeter absorber (in GeV) for 2, 10, 50 and 300 GeV incident muons (MC results). Here the real energy deposited in each component of the calorimeter is given, without correcting for the respective sampling fraction nor normalization to experimental data. The MC results were simulated in a spot of 1 mm, see text for details.

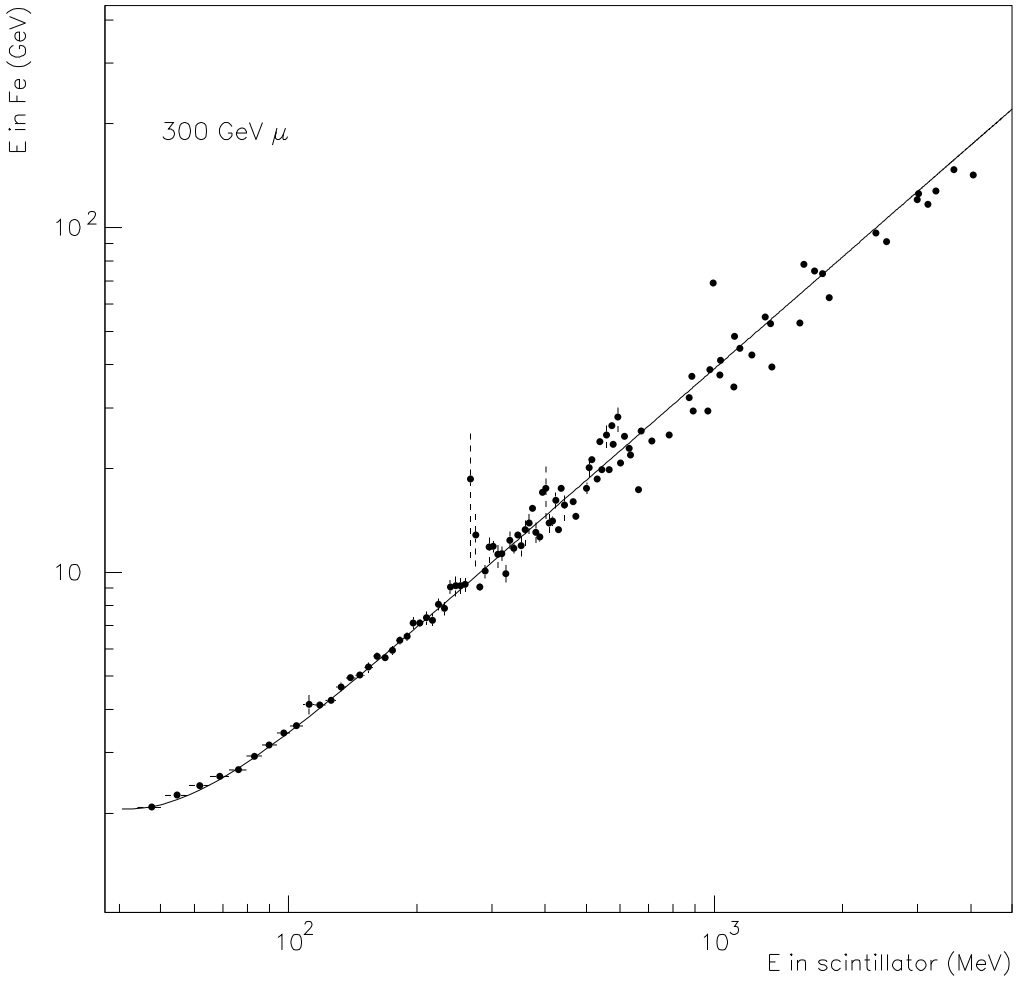

Figure 9: The energy loss in the scintillator as a function of the energy loss in the Tile calorimeter absorber (iron) for 300 GeV incident muons (MC results). The full curve is a parameterization to the data. Here the real energy deposited in each component of the calorimeter is given, without correcting for the respective sampling fraction nor normalization to experimental data. The MC results were simulated in a spot of 1 mm, see text for details.

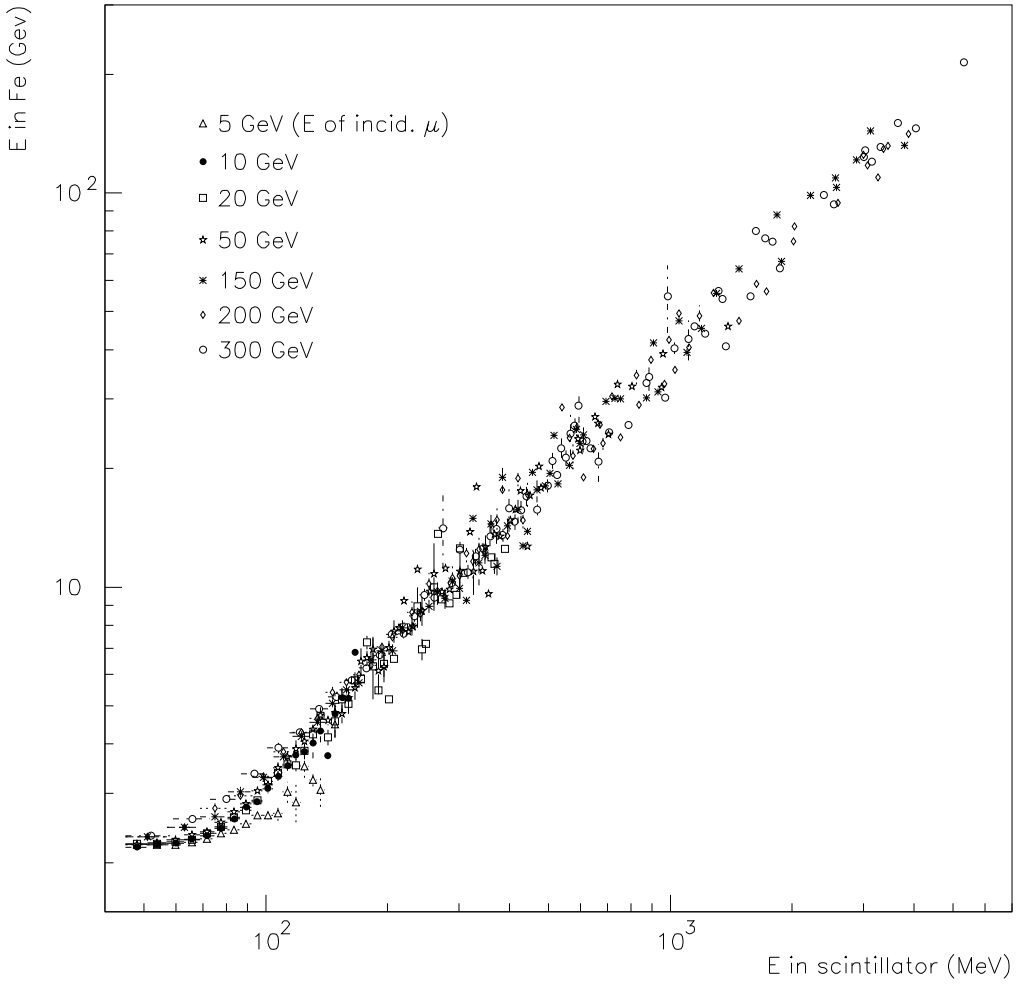

Figure 10: The energy loss in the scintillator (in MeV) as a function of the energy loss in the Tile calorimeter absorber (in GeV) for several incident muon energies. Here the real energy deposited in each component of the calorimeter is given, without correcting for the respective sampling fraction nor normalization to experimental data. The MC results were simulated in a spot of 1 mm, see text for details.

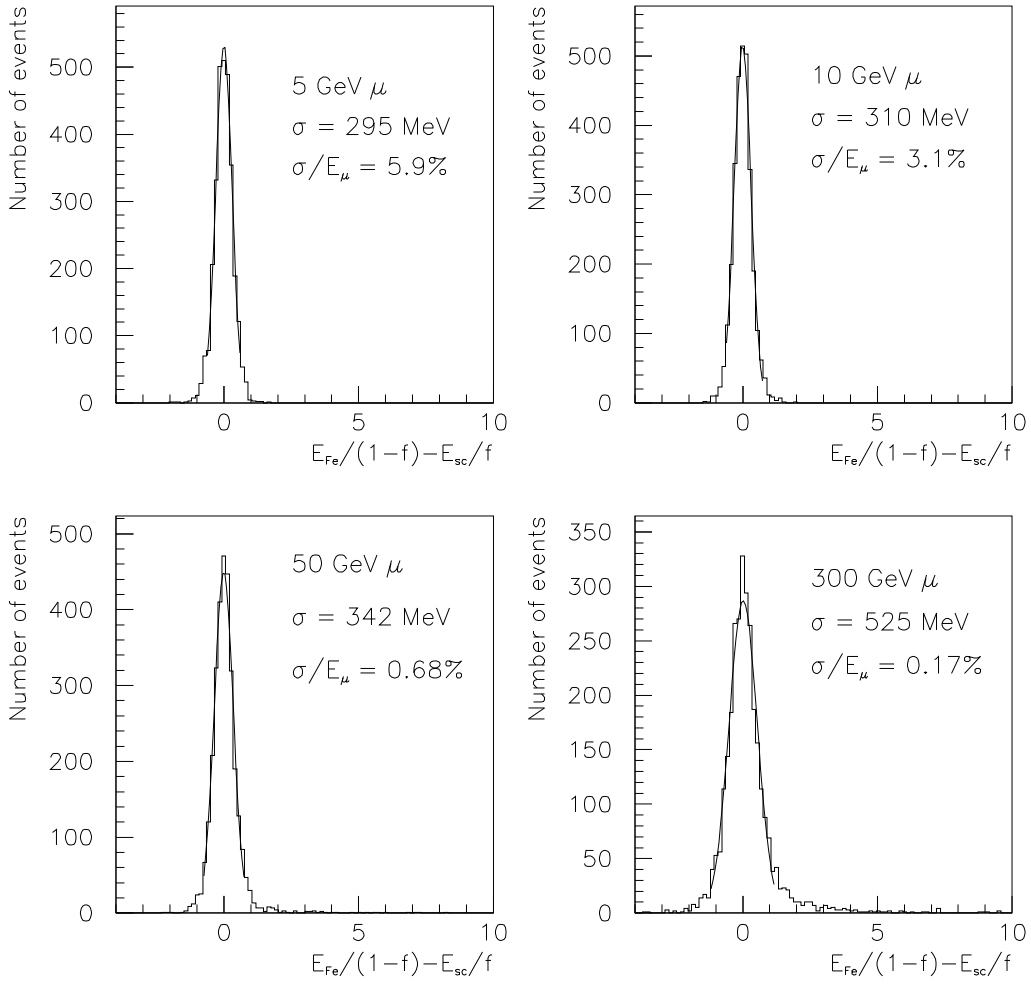

Figure 11: The difference of the energy loss in the Tile calorimeter absorber corrected for the sampling fraction in iron and the energy loss in the scintillator corrected for the sampling fraction in the scintillator. The MC events were simulated in a spot of 1 mm, see text for details.

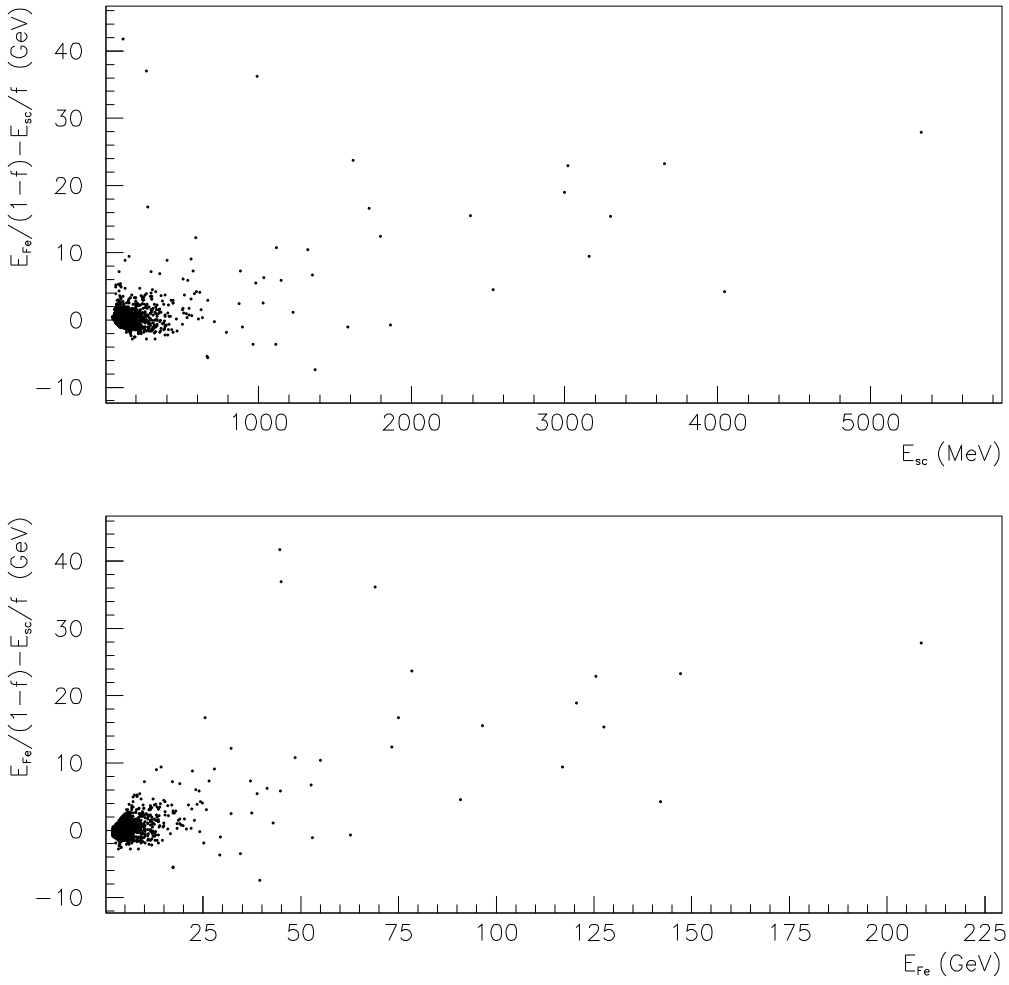

Figure 12: The difference of the energy loss in the Tile calorimeter absorber and the energy loss in the scintillator corrected for the respective sampling fractions as a function of (a) the energy deposited in scintillator, (b) the energy deposited in iron for 300 GeV muons. The MC events were simulated with an impact point of 1 mm, see text for details.

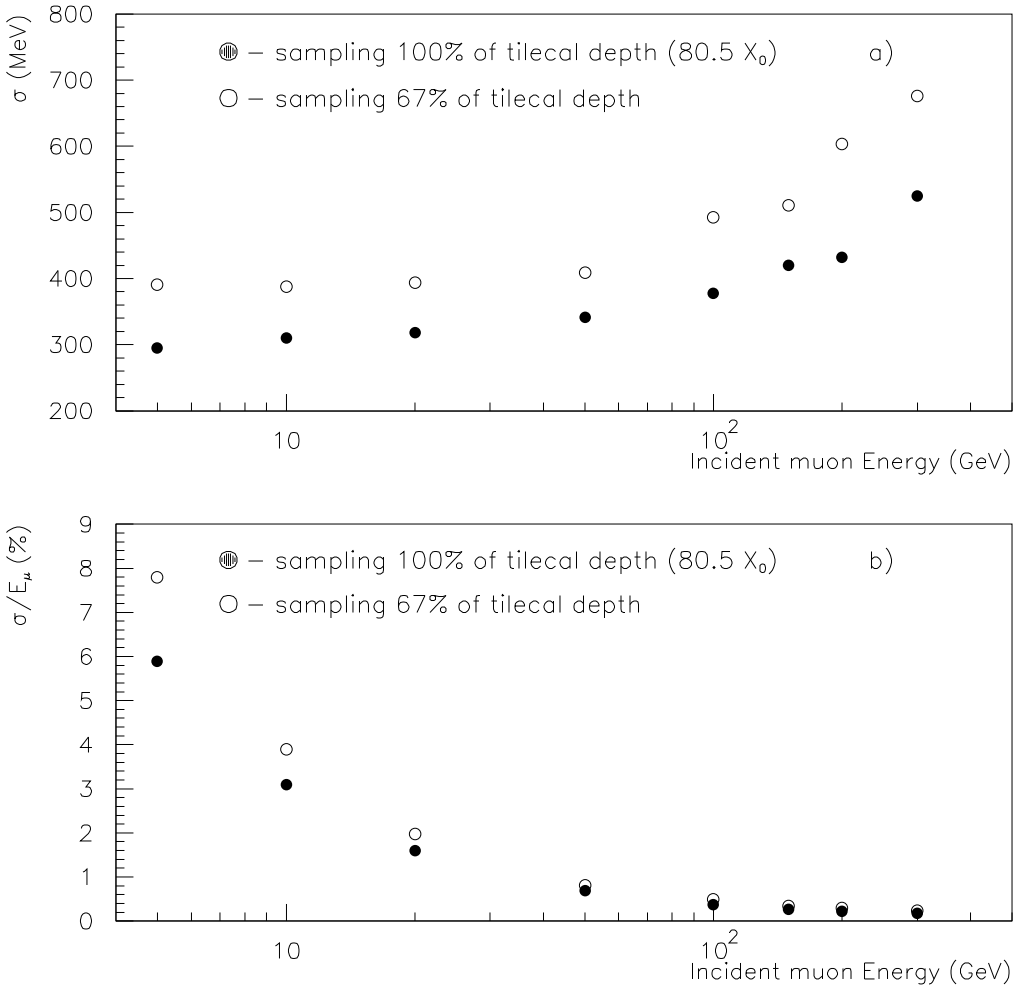

Figure 13: The spread (σ) of the energy loss estimated in the Tile calorimeter (Fe + scintillator) by muons of incident energy between 5 and 300 GeV. The σ as obtained from a Gaussian fit within ± 2 σ is given (a) in MeV, (b) divided by the incident muon energy (σ/E_μ), sampled over the full calorimeter depth of 80.5 X_0 (black dots) and sampled only over 67% of the active calorimeter depth (open circles) with respect to the total energy loss in the calorimeters. The MC events were simulated with an impact point of 1 mm, see text for details.

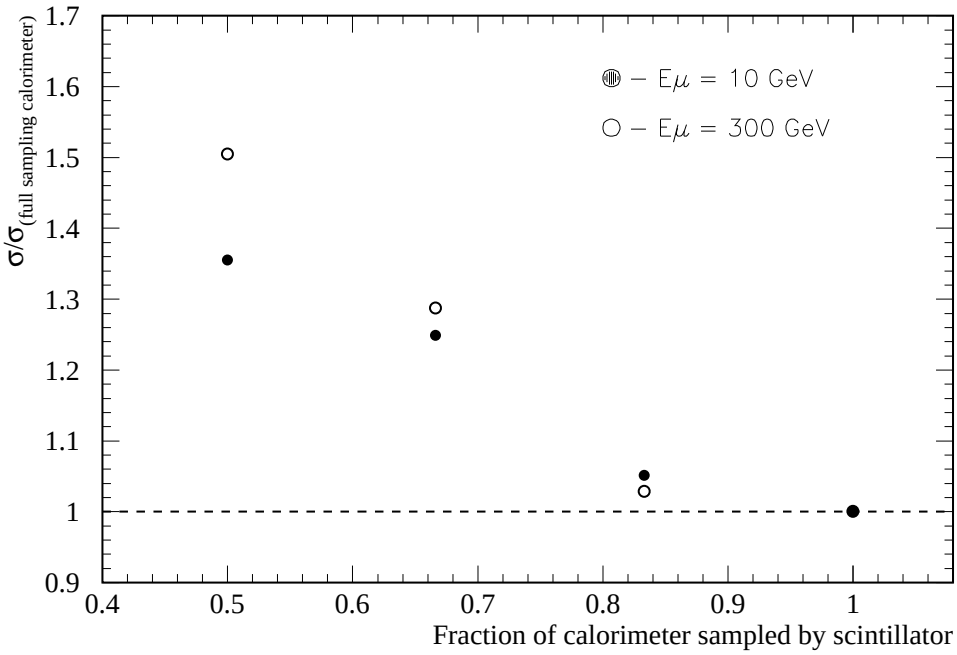

Figure 14: The resolution (σ) on the estimation of the energy loss in the Tile calorimeter as a function of the fraction of the calorimeter which is sampled by the scintillator. The resolution is given for 10 and 300 GeV muons and is normalized to the resolution obtained with full calorimeter sampling (80.5 X_0). The MC events were simulated with an impact point of 1 mm, see text for details.

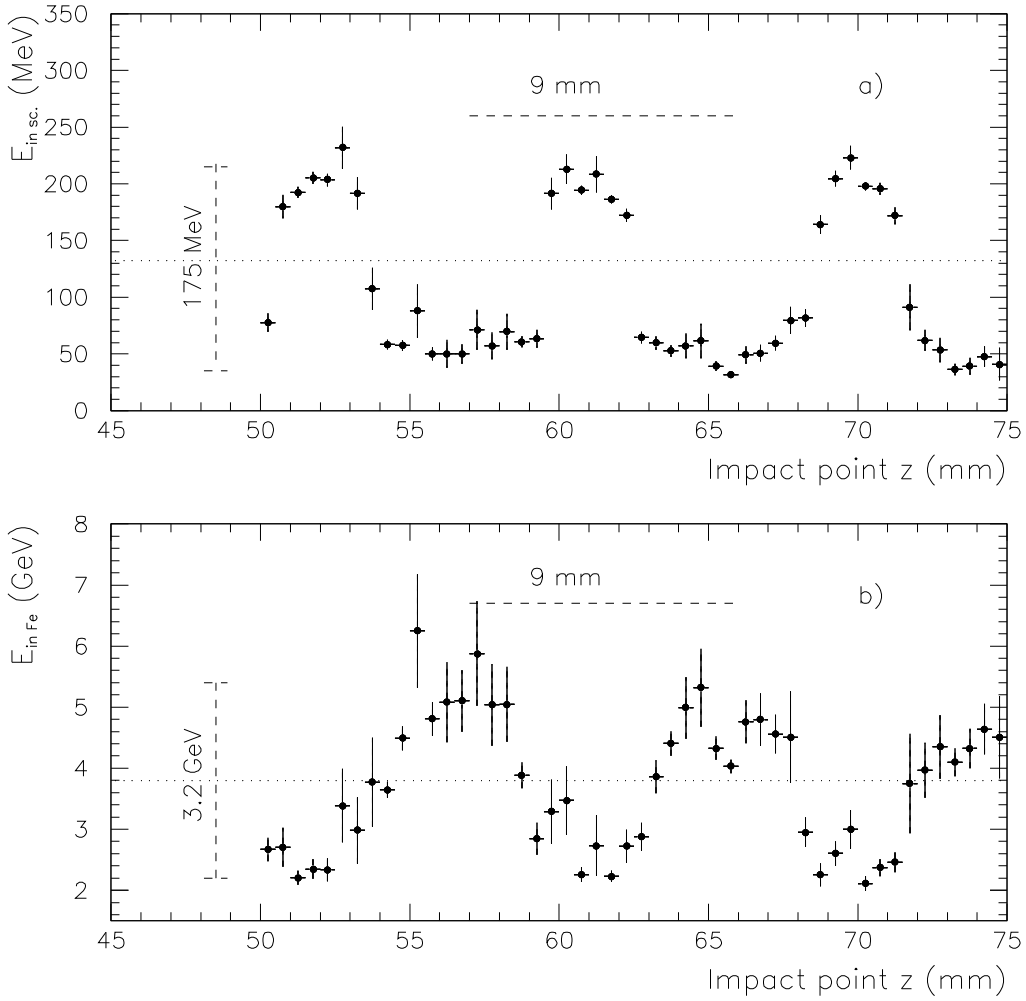

Figure 15: The energy deposited (a) in scintillator (b) in the iron as a function of the Tile calorimeter z impact point for 180 GeV muons ($\theta = 0^o$). The MC results show the exact amount of energy deposited in each component without correcting for the sampling fraction.

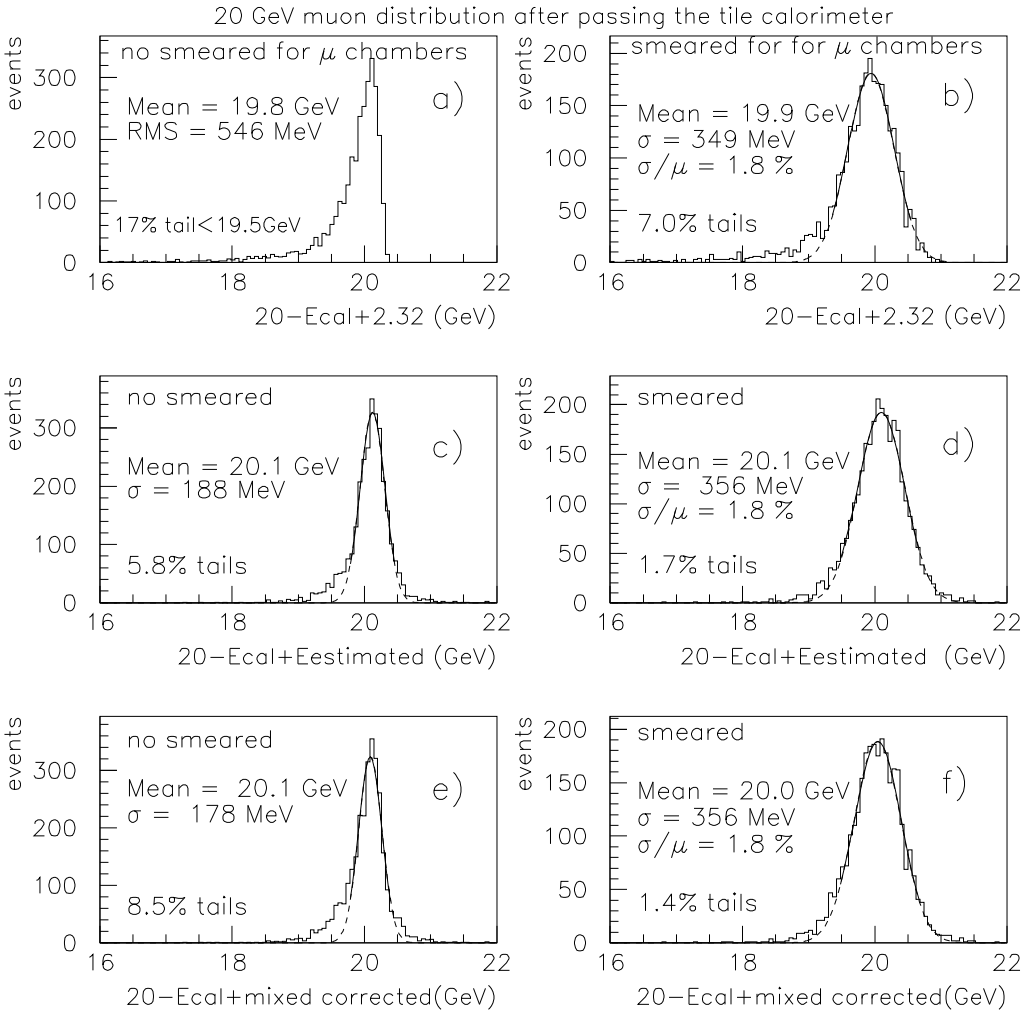

Figure 16: The expected energy distribution for 20 GeV muons after traversing the Tile calorimeter prototype using different methods to correct for the energy losses in the calorimeter. Method 1 adds to each event the most probable value of the energy lost in the calorimeter (peak = 2.32 GeV) (a) before smearing, (b) after smearing for the contribution of the multiple scattering and the measurement/alignement error in the muon chambers. Method 2 corrects on the event-to-event basis for the energy loss in the calorimeter (c) before smearing, (d) after smearing. Method 3 is a mixture of the 2 first methods, i.e. use method 1 for events with $E_{scintillator} \leq 80$ MeV and method 2 for events with $E_{scintillator}$ above 80 MeV (e) before smearing, (f) after smearing.

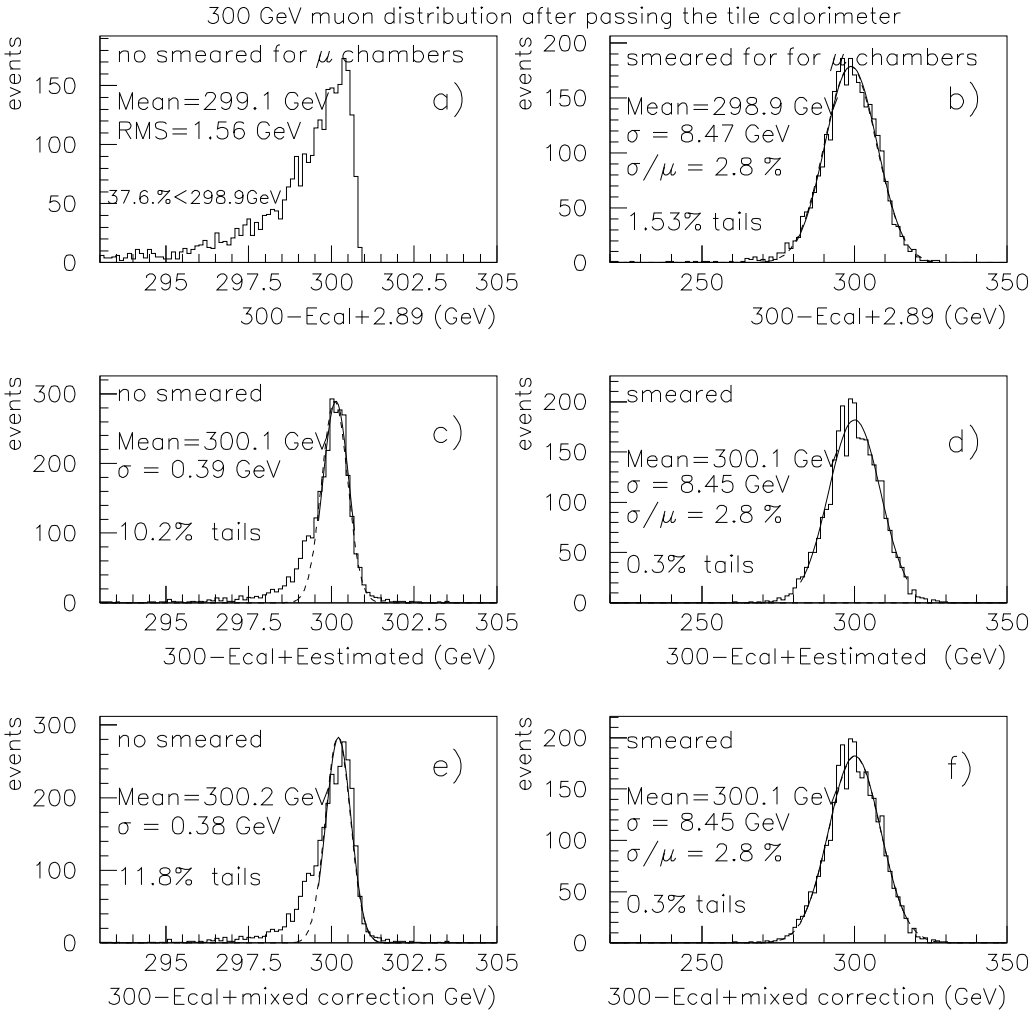

Figure 17: The expected energy distribution for 300 GeV muons after traversing the Tile calorimeter prototype using different methods to correct for the energy losses in the calorimeter. Method 1 adds to each event the most probable value of the energy lost in the calorimeter (peak = 2.89 GeV) (a) before smearing, (b) after smearing for the contribution of the multiple scattering and the measurement/alignement error in the muon chambers. Method 2 corrects on the event-to-event basis for the energy loss in the calorimeter (c) before smearing, (d) after smearing. Method 3 is a mixture of the 2 first methods, i.e. use method 1 for events with $E_{scintillator} \leq 80$ MeV and method 2 for events with $E_{scintillator}$ above 80 MeV (e) before smearing, (f) after smearing.

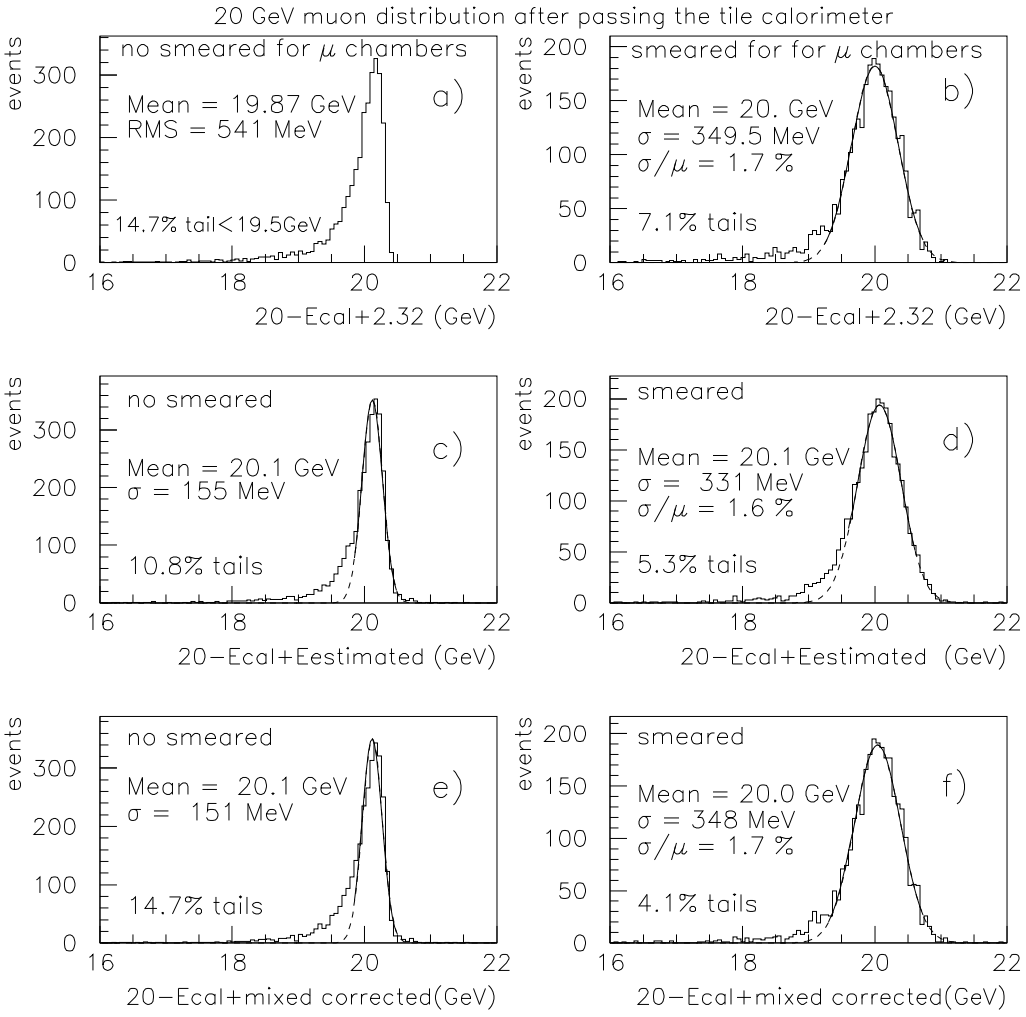

Figure 18: The expected energy distribution for 20 GeV muons after traversing the Tile calorimeter prototype but reading only 67% of the scintillator information. Different methods were used to correct for the energy losses in the calorimeter. Method 1 adds to each event the most probable value of the energy lost in the calorimeter (peak = 2.32 GeV) (a) before smearing, (b) after smearing for the contribution of the multiple scattering and the measurement/alignement error in the muon chambers. Method 2 corrects on the event-to-event basis for the energy loss in the calorimeter (c) before smearing, (d) after smearing. Method 3 is a mixture of the 2 first methods, i.e. use method 1 for events with $E_{scintillator} \leq 60$ MeV and method 2 for events with $E_{scintillator}$ above 60 MeV (e) before smearing, (f) after smearing.